



Reeb's Theorem and Periodic Orbits for a Rotating Hénon–Heiles Potential

V. Lanchares¹ · A. I. Pascual¹ · M. Iñarrea² · J. P. Salas² · J. F. Palacián³ · P. Yanguas³

Received: 19 July 2019 / Revised: 9 November 2019
© Springer Science+Business Media, LLC, part of Springer Nature 2019

Abstract

We apply Reeb's theorem to prove the existence of periodic orbits in the rotating Hénon–Heiles system. To this end, a sort of detuned normal form is calculated that yields a reduced system with at most four non degenerate equilibrium points. Linear stability and bifurcations of equilibrium solutions mimic those for periodic solutions of the original system. We also determine heteroclinic connections that can account for transport phenomena.

Keywords Averaging · Normalization · Reduced space · Hamiltonian oscillators · Periodic solutions

1 Introduction

Hénon–Heiles system arises as a model to answer the question of the existence of a third integral of motion in an axisymmetrical potential [13]. It was formulated in the context of

✉ V. Lanchares
vlancha@unirioja.es

A. I. Pascual
aipasc@unirioja.es

M. Iñarrea
manuel.inarrea@unirioja.es

J. P. Salas
josepablo.salas@unirioja.es

J. F. Palacián
palacian@unavarra.es

P. Yanguas
yanguas@unavarra.es

¹ Departamento de Matemáticas y Computación, Universidad de La Rioja, 26006 Logroño, La Rioja, Spain

² Área de Física Aplicada, Universidad de La Rioja, 26006 Logroño, La Rioja, Spain

³ Departamento de Estadística, Informática y Matemáticas and Institute for Advanced Materials, Universidad Pública de Navarra, 31006 Pamplona, Spain

galactic dynamics, although the potential chosen does not necessarily represent an actual galactic one. However, it is simple enough to account for many qualitative aspects of similar, but more complex, dynamical systems. For instance, it serves as a good model to study escape dynamics [4] which, in turn, provides a mechanism to describe reaction dynamics with some open channels [15]. Moreover, also in the context of atomic physics, Hénon–Heiles system can be used as a suitable model for ion traps, where a confinement region is created by means of external fields [16].

Nevertheless, both in the field of atomic physics and in the field of galactic dynamics, rotating potentials are of great interest. Indeed, the addition of a magnetic field or a circularly polarized microwave field to a Rydberg atom introduces a Coriolis term, giving rise to a rotating potential of Hénon–Heiles type [29]. This model describes properly the chaotic ionization mechanism in chemical reactions. On the other hand, in the context of galactic dynamics, the classical book by Binney and Tremaine [3] emphasizes the necessity of considering rotating potentials to better explain the dynamics of the stellar orbits in a galaxy. In this setting equilibrium points and periodic orbits play an important role, as they organize the phase flow structure and different qualitative aspects of the dynamical system can be understood. An interesting example is the possibility of matter transfer through heteroclinic connections between equilibrium points, a mechanism proposed to explain the formation of spiral arms [31]. Nevertheless, the general interest lies in the determination of periodic orbits, mainly used to classify different types of motion that can account, for instance, for the existence of unusual rotating barred galaxies [27].

In this paper, we consider the system given by

$$\mathcal{H} = \frac{1}{2}(X^2 + Y^2) - \omega(xY - yX) + \frac{1}{2}(x^2 + y^2) + ax^2 + by^3, \quad (1)$$

which can be viewed as a generalized Hénon–Heiles system in a rotating reference frame with angular velocity ω and it can serve as a model for chemical reactions and galactic dynamics. The system depends on three parameters, namely a , b and ω . The rotating frequency, ω , controls in a great deal the structure of the phase space, modifying the stability properties of equilibrium points when the critical value $\omega = 1$ is crossed [14]. Our main goal is to establish the existence of periodic orbits and bifurcations in a vicinity of the origin when ω is close to the critical value.

Averaging method [32,35] is suitable for this purpose. Indeed, it has been extensively used to determine periodic orbits in both non rotating [1,5,6,18–20] and rotating potentials [8,9] and also to establish periodic orbits for system (1), as it is done in [17]. The method is simple to apply, although some times tricky, but, if the system is Hamiltonian, alternative techniques can be used. In this sense, suppose that the Hamiltonian is divided into an unperturbed part and a perturbation, the solutions of the unperturbed system being periodic. Then, the unperturbed Hamiltonian can be extended as a formal integral, decreasing the number of degrees of freedom of the system by one unit, using normal form theory combined with symplectic reduction. The equilibrium points of the reduced system are associated to families of periodic orbits of the perturbed one, i.e. the full system. This is in essence Reeb’s theorem [30] which, combined with symplectic reduction, is in many aspects equivalent to the averaging method, but preferable as all the periodic orbits obtained are different. As well, it works properly in some degenerate situations. More specifically, symplectic reduction provides the right way of obtaining the base space (or reduced space) in terms of a fixed value of \mathcal{H}_0 (the unperturbed Hamiltonian), say h . This space can be a symplectic manifold (regular reduction) or an orbifold (singular reduction) but can be parameterized by global coordinates, the so called invariants of the reduction process, see for instance [36]. This allows us to analyze the

dynamics of the reduced system in the reduced space properly. We will use this approach to prove the existence of periodic orbits for the Hamiltonian system defined by (1).

The paper is organized as follows. In Sect. 2 we introduce some general properties of the system, focusing on the linear approximation in a vicinity of the origin. In Sect. 3, Reeb’s theorem is presented, the normal form around the origin is computed to first order and symplectic reduction is executed. Section 4 is devoted to the statement of the main results about the existence of periodic orbits, in particular Theorems 3, 4, 5 and 6. In Sect. 5, bifurcations of relative equilibria are related with the bifurcations of the families of periodic orbits by means of Poincaré surfaces of section. Moreover, by applying some theorems that reconstruct the flow of the full system associated with the different bifurcations of the relative equilibria, we establish the occurring bifurcations of the families of periodic solutions. This is summarized in Theorem 7, our last main result.

We want to emphasize that our normalization and reduction procedures are somehow non standard due to the fact that we are mainly interested in values of the rotating frequency, ω , near 1. Thus, to succeed in our approach we do not consider the 1:1 resonance combined with the Coriolis term existing in the unperturbed part of the Hamiltonian function, and perform a different approach to compute the average and reduce the truncated averaged system, as we will see in Sect. 3.

2 The System

We start by setting some properties of the Hamiltonian system corresponding to (1). The equations of motion are given by

$$\begin{aligned} \dot{x} &= \frac{\partial \mathcal{H}}{\partial X} = X + \omega y, & \dot{X} &= -\frac{\partial \mathcal{H}}{\partial x} = -x + \omega Y - 2axy, \\ \dot{y} &= \frac{\partial \mathcal{H}}{\partial Y} = Y - \omega x, & \dot{Y} &= -\frac{\partial \mathcal{H}}{\partial y} = -y - \omega X - ax^2 - 3by^2. \end{aligned} \tag{2}$$

It is worth noting that the system enjoys some symmetries. Indeed, \mathcal{H} remains invariant under the transformations

$$\begin{aligned} \mathcal{H}(x, y, X, Y; \omega, a, b) &= \mathcal{H}(x, y, -X, -Y; -\omega, a, b), \\ \mathcal{H}(x, y, X, Y; \omega, a, b) &= \mathcal{H}(-x, y, X, -Y; \omega, a, b), \\ \mathcal{H}(x, y, X, Y; \omega, a, b) &= \mathcal{H}(x, -y, -X, Y; \omega, -a, -b). \end{aligned} \tag{3}$$

The first symmetry allows us to restrict the study to the case $\omega > 0$. Indeed, let

$$\Phi(t) = (x(t), y(t), X(t), Y(t))$$

be a solution of the differential system (2) for $\omega > 0$, then

$$(x(-t), y(-t), -X(-t), -Y(-t))$$

is a solution for $\omega < 0$. The second symmetry tells us that, if $\Phi(t)$ is a solution of the Hamiltonian differential system (2), then

$$(-x(-t), y(-t), X(-t), -Y(-t))$$

is also a solution of the same system. That is, the phase flow is time reversal symmetric with respect to the y axis. As a consequence, equilibrium points are located symmetrically with respect to the y axis in the configuration space. Moreover, periodic orbits are either

symmetric with respect to the y axis or they appear in pairs, which are symmetric respect to the y axis. Finally, the third symmetry indicates that it is enough to consider either the case $a \geq 0$ or the case $b \geq 0$. In fact, if $\Phi(t)$ is a solution of (2) for a pair of values (a, b) , then

$$(x(-t), -y(-t), -X(-t), Y(-t))$$

is a solution when the pair is replaced by $(-a, -b)$.

Another interesting quasi-symmetry of the system emerges when studying equilibrium points. Suppose that

$$E_0 \equiv (x_0, y_0, X_0, Y_0)$$

is an equilibrium point for $\omega = \omega_0$, then

$$\hat{E}_0 \equiv (-x_0/\omega_0^2, -y_0/\omega_0^2, -X_0/\omega_0^4, -Y_0/\omega_0^4)$$

is also an equilibrium point for $\omega = 1/\omega_0$. In some sense, there is a correspondence between the situations $0 < \omega < 1$ and $\omega > 1$. However, there is a slight difference. Indeed, equilibrium points are related to the critical points of the effective potential

$$\Phi_{\text{eff}} = \mathcal{H} - \frac{1}{2}(\dot{x}^2 + \dot{y}^2) = \frac{1}{2}(1 - \omega^2)(x^2 + y^2) + y(ax^2 + by^2), \quad (4)$$

in such a way that if E_0 is an equilibrium point of the system (2), then (x_0, y_0) is a critical point of the effective potential Φ_{eff} . It can be seen that, if E_0 is a minimum (maximum) of the effective potential, then \hat{E}_0 is a maximum (minimum) of Φ_{eff} . In the case E_0 is a saddle point, the same happens for \hat{E}_0 . As a consequence, linear stability properties cannot be extended directly from the case $0 < \omega < 1$ to the case $\omega > 1$, if the corresponding critical point is a minimum (maximum). While a minimum of Φ_{eff} is always a linear stable equilibrium, the same cannot be said for a maximum. A detailed study of equilibrium points of this system and their stability properties is given in [14], where it is established that the maximum number of equilibrium points is 4, the origin being one of them for every value of the parameters.

If we pay attention to the eigenvalues of the linear system at the origin, we find that they are

$$\lambda_{1,2} = \pm i(\omega - 1), \quad \lambda_{3,4} = \pm i(\omega + 1), \quad (5)$$

and it is always a center, provided $\omega \neq 1$. However, just at $\omega = 1$, there is a pair of zero eigenvalues and the elliptic character is lost, which indicates the appearance of a bifurcation. In fact, all the existing equilibrium points coalesce. Moreover, in the passage from $0 < \omega < 1$ to $\omega > 1$, the origin changes from a minimum to a maximum of the effective potential.

Another interesting feature is that, in a vicinity to the origin, the system can be viewed as two perturbed harmonic oscillators with frequencies $|\omega - 1|$ and $\omega + 1$. Thus, if $\omega \approx 1$, one of them oscillates fast in comparison to the other and the theory of averaging is suitable to study the existence of periodic solutions. This will be our goal, to prove the existence of periodic orbits and their bifurcations in a vicinity of the origin when $\omega \approx 1$, that is, close to the transition case.

3 Averaging and Normal Form

The averaging theory is a classical topic in the field of differential equations (see for instance [32,35]) and has been used satisfactorily for the determination of periodic orbits in a great

variety of dynamical systems. However, for Hamiltonian systems, Reeb’s theorem provides an alternative framework to prove the existence of periodic solutions [23,36].

Let (M, Ω) be a symplectic manifold of dimension $2n$ and consider a Hamiltonian system of the form

$$\mathcal{H} = \mathcal{H}_0 + \varepsilon\mathcal{H}_1,$$

where $\mathcal{H}_0, \mathcal{H}_1 : M \rightarrow \mathbb{R}$ are smooth functions and ε a real small parameter. Let us assume that, for $\varepsilon = 0$, there is an interval $\mathbb{I} \subset \mathbb{R}$ such that, for each $h \in \mathbb{I}$, the solutions of the Hamiltonian system are periodic with period $T(h)$. Indeed, it is supposed that, for the Hamiltonian vector field $Y_0 = (d\mathcal{H}_0)^\#$ with symplectic flow ϕ_0^t , the set $\mathcal{N}_0(h) = \mathcal{H}_0^{-1}(h)$ is a connected circle bundle over a base space (i.e., the reduced space) $B(h)$, for each $h \in \mathbb{I}$. Moreover, we consider the projection $\pi : \mathcal{N}_0(h) \rightarrow B(h)$. Thus, the following result can be proved in this context:

Theorem 1 *The base space $B(h)$ inherits, from (M, Ω) , a symplectic structure ϖ ; i.e., $(B(h), \varpi)$ is a symplectic manifold.*

Now, consider the Hamiltonian vector field $Y_\varepsilon = Y_0 + \varepsilon Y_1 = d\mathcal{H}_\varepsilon^\#$ with symplectic flow ϕ_ε^t and the set $\mathcal{N}_\varepsilon(h) = \mathcal{H}_\varepsilon^{-1}(h)$. Let the average of \mathcal{H}_1 be

$$\bar{\mathcal{H}} = \frac{1}{T} \int_0^T \mathcal{H}_1(\phi_0^t) dt,$$

which is a smooth function on $B(h)$, and let $\bar{\phi}^t$ be the flow on $B(h)$ defined by $\bar{Y} = d\bar{\mathcal{H}}^\#$. A critical point of $\bar{\mathcal{H}}$ is *nondegenerate* if the Hessian at the critical point is nonsingular. Reeb’s theorem can be formulated as:

Theorem 2 *If $\bar{\mathcal{H}}$ has a nondegenerate critical point at $\pi(p) = \bar{p} \in B$ with $p \in \mathcal{N}_0$, then there are smooth functions $p(\varepsilon)$ and $T(\varepsilon)$ for ε small with $p(0) = p$, $T(0) = T$, $p(\varepsilon) \in \mathcal{N}_\varepsilon$, and the solution of Y_ε through $p(\varepsilon)$ is $T(\varepsilon)$ -periodic.*

To apply Theorem 2, the first step is to convert the Hamiltonian function into an equivalent one made of two coupled harmonic oscillators with frequencies $|1 - \omega|$ and $1 + \omega$. To achieve it, we transform the system by means of the canonical change of variables

$$\begin{aligned} x &= -\frac{x_1}{\sqrt{2}} + \frac{x_2}{\sqrt{2}}, & X &= -\frac{X_1}{\sqrt{2}} + \frac{X_2}{\sqrt{2}}, \\ y &= \frac{X_1}{\sqrt{2}} + \frac{X_2}{\sqrt{2}}, & Y &= -\frac{x_1}{\sqrt{2}} - \frac{x_2}{\sqrt{2}}. \end{aligned} \tag{6}$$

The transformed Hamiltonian is given by

$$\begin{aligned} \mathcal{H} &= \frac{1}{2}(1 - \omega)(x_1^2 + X_1^2) + \frac{1}{2}(1 + \omega)(x_2^2 + X_2^2) \\ &+ \frac{X_1 + X_2}{2\sqrt{2}} (a(x_1 - x_2)^2 + b(X_1 + X_2)^2). \end{aligned} \tag{7}$$

Taking into account that $\omega \approx 1$, the quadratic part of the Hamiltonian corresponds to two harmonic oscillators with widely separated frequencies. This situation has been considered by Tuwankotta and Verhulst [34], who applied averaging techniques to compute the normal form. The key idea consists in considering the term with almost zero frequency as part of the perturbation. In fact, the quadratic part of Hamiltonian (7) is no more than a detuned harmonic

oscillator in 1:0 resonance. It can be decomposed into two parts. One corresponding to the pure resonance, which accounts for fast oscillations, and the other one corresponding to the *detuned* part, associated to the slow oscillations. The detuned part is incorporated to the perturbation and the pure resonant term is extended as a first integral, up to a certain order, by means of normal form theory. Detuning is a useful technique to study the properties of near resonant systems and has been applied to different models in galactic dynamics [10,11,28] and also in atomic physics [16].

To properly apply the averaging or normalization procedure, and taking into account that $\omega \approx 1$, we introduce the scaling

$$1 - \omega = \varepsilon\nu, \quad x_j = \varepsilon x_j, \quad X_j = \varepsilon X_j, \quad j = 1, 2,$$

where ν is a new parameter and ε is introduced to highlight that $1 - \omega$ and the variables x_j, X_j are of the same order of smallness. If \mathcal{H} is also scaled by a factor ε^{-2} , we arrive at

$$\begin{aligned} \mathcal{H} = & \frac{1}{2}(1 + \omega)(x_2^2 + X_2^2) \\ & + \varepsilon \left[\frac{1}{2}\nu(x_1^2 + X_1^2) + \frac{X_1 + X_2}{2\sqrt{2}} (a(x_1 - x_2)^2 + b(X_1 + X_2)^2) \right]. \end{aligned} \tag{8}$$

Hamiltonian (8) is in the form of Reeb’s theorem with

$$\begin{aligned} \mathcal{H}_0 &= \frac{1}{2}(1 + \omega)(x_2^2 + X_2^2), \\ \mathcal{H}_1 &= \frac{1}{2}\nu(x_1^2 + X_1^2) + \frac{X_1 + X_2}{2\sqrt{2}} (a(x_1 - x_2)^2 + b(X_1 + X_2)^2). \end{aligned} \tag{9}$$

Fixed $h = \mathcal{H}_0 \geq 0$, the set $\mathcal{N}_0(h) = \mathcal{H}_0^{-1}(h)$ is diffeomorphic to $S^1 \times \mathbb{R}^2$, a connected circle bundle, the base space $B(h)$ being \mathbb{R}^2 , see [26]. Setting $\varepsilon = 0$, and taking $h > 0$, all the solutions are periodic with period $2\pi/(1 + \omega)$ and are given by

$$\left(x_1^0, \sqrt{\frac{2h}{1 + \omega}} \sin(1 + \omega)t, X_1^0, \sqrt{\frac{2h}{1 + \omega}} \cos(1 + \omega)t \right). \tag{10}$$

The next step in applying Reeb’s theorem involves the average of \mathcal{H}_1 . We can proceed in different manners to obtain $\bar{\mathcal{H}}_1$. The most direct approach is to introduce polar coordinates for the unperturbed part \mathcal{H}_0 ,

$$x_2 = \sqrt{2r_2} \sin \theta_2, \quad X_2 = \sqrt{2r_2} \cos \theta_2,$$

and average \mathcal{H}_1 over the angle θ_2 , that is

$$\bar{\mathcal{H}}_1 = \frac{1}{2\pi} \int_0^{2\pi} \mathcal{H}_1 d\theta_2 = \frac{1}{2}\nu(x_1^2 + X_1^2) + \frac{X_1}{2\sqrt{2}} (a(x_1^2 + c) + b(X_1^2 + 3c)), \tag{11}$$

where $c = r_2 = h/(1 + \omega)$ is taken to be constant and it is related to the amplitude of the periodic solutions for $\varepsilon = 0$.

Another way to obtain the average is by means of the reduction theory for polynomial Hamiltonians [25,26]. Indeed, it is required that \mathcal{H}_0 is a formal integral up to first order. If \mathcal{H}_1 is decomposed into the sum

$$\mathcal{H}_1 = \mathcal{K}_1 + \tilde{\mathcal{H}}_1,$$

the normal form, up to order one (truncating higher-order terms), is given by \mathcal{K}_1 , provided that the Poisson bracket $\{\mathcal{K}_1, \mathcal{H}_0\}$ is equal to 0. By introducing complex canonical variables

$$x_k = \frac{1}{\sqrt{2}}(u_k + iv_k), \quad X_k = \frac{i}{\sqrt{2}}(u_k - iv_k), \quad k = 1, 2,$$

\mathcal{K}_1 is given by those monomials, $u_1^{\alpha_1} u_2^{\alpha_2} v_1^{\beta_1} v_2^{\beta_2}$, such that $\alpha_2 = \beta_2$. It is easy to check that $\mathcal{K}_1 = \tilde{\mathcal{H}}_1$. However, this approach has the flavor of a versal normal form [2], that is a normal form around an equilibrium point when the canonical form of the linearized part depends on parameters (in our case, this parameter is the frequency ω). We stress that the normal form is also valid for the critical case $\omega = 1$, which is the essence of versal normal forms. Due to this fact, they have been used to study some interesting dynamical systems. For instance, the dynamics around the Lagrangian point L_4 in the circular restricted three body problem near the critical mass ratio [7,33]. In addition, if pushing the average procedure to higher orders is required, normal forms can be computed in an algorithmic manner by means of Lie transforms.

In summary, after the averaging procedure or after computing the normal form, up to first order, we are left with a reduced Hamiltonian system of one degree of freedom defined in the reduced space $B(h) = \mathbb{R}^2$ given by the Hamiltonian function

$$\mathcal{K} = \mathcal{K}_1 = \tilde{\mathcal{H}}_1 = \frac{1}{2}v(x_1^2 + X_1^2) + \frac{X_1}{2\sqrt{2}}(a(x_1^2 + c) + b(X_1^2 + 3c)), \tag{12}$$

depending on the four parameters v, a, b and c .

4 Relative Equilibria and Periodic Orbits

It is worth noting that Hamiltonian (12) is no more than a scaled version of the effective potential (4) when $c = 0$. For c small enough, we will obtain the same number of equilibrium points and the same bifurcation pattern than the observed for the original system. We distinguish two cases. On the one hand, if $a = 0$ the reduced Hamiltonian \mathcal{K} depends on v, b and c and it is converted into

$$\mathcal{K} = \frac{1}{2}v(x_1^2 + X_1^2) + \frac{bX_1}{2\sqrt{2}}(X_1^2 + 3c). \tag{13}$$

We can establish the following result.

Theorem 3 *Let us consider the Hamiltonian system defined by (8) when $a = 0, \omega \approx 1$ and let \mathcal{K} be its average. Then, if $b \neq 0$ and h is small enough (i.e. c small enough), there exist two families of periodic orbits, parameterized by h , provided*

$$2v^2 - 9b^2c > 0.$$

In the case the inequality reverses, there are not periodic orbits.

Proof The equations of motion for the averaged system are

$$\begin{aligned} \dot{x}_1 &= vX_1 + \frac{3b}{2\sqrt{2}}(X_1^2 + c), \\ \dot{X}_1 &= -vX_1. \end{aligned} \tag{14}$$

By setting the equations to zero, the equilibrium points result to be

$$E_{1,2} \equiv \left(0, \frac{-2v \pm \sqrt{2v^2 - 9b^2c}}{3b} \right). \tag{15}$$

Thus, if $2v^2 - 9b^2c > 0$, two non degenerate equilibria exist and, applying Theorem 2, there exist two periodic orbits. \square

On the other hand, when $a \neq 0$, a proper scaling allows us to reduce the number of parameters. Indeed, if \mathcal{K} is multiplied by a^2 , we get

$$a^2\mathcal{K} = \frac{1}{2}v((ax_1)^2 + (aX_1)^2) + \frac{(aX_1)}{2\sqrt{2}} \left((ax_1)^2 + a^2c + \frac{b}{a}((aX_1)^2 + 3a^2c) \right).$$

Thus, renaming the variables and the parameters according to

$$x_1 \rightarrow ax_1, \quad X_1 \rightarrow aX_1, \quad c \rightarrow a^2c, \quad b \rightarrow b/a, \quad \mathcal{K} \rightarrow a^2\mathcal{K},$$

we obtain

$$\mathcal{K} = \frac{1}{2}v(x_1^2 + X_1^2) + \frac{X_1}{2\sqrt{2}}(x_1^2 + c + b(X_1^2 + 3c)), \tag{16}$$

depending again on v, b and c . If this scaling was made from the very beginning, the reduced Hamiltonian (16) would come from the averaging of Hamiltonian

$$\mathcal{H} = \frac{1}{2}(X^2 + Y^2) - \omega(xY - yX) + \frac{1}{2}(x^2 + y^2) + yx^2 + by^3, \tag{17}$$

which is Hamiltonian (1) when $a = 1$.

On what follows, we will restrict ourselves to the case $a \neq 0$ with averaged Hamiltonian \mathcal{K} given by (16), coming from the starting Hamiltonian (17) with $a = 1$. The following results can be stated.

Theorem 4 *Let us consider the Hamiltonian system defined by (17) when $\omega \approx 1$ and let \mathcal{K} , given by (16), its average. Then, if $b \neq 0$ and h is small enough (i.e. c small enough):*

1. *There are four families of periodic orbits, parameterized by h , if*

$$(4 - 6b)v^2 - (1 + 3b)c > 0 \quad \text{and} \quad 4v^2 - 6(1 + 3b)bc > 0.$$

2. *There are two families of periodic orbits, parameterized by h , if*

$$((4 - 6b)v^2 - (1 + 3b)c)(4v^2 - 6(1 + 3b)bc) < 0.$$

3. *There are no periodic orbits if*

$$(4 - 6b)v^2 - (1 + 3b)c < 0 \quad \text{and} \quad 4v^2 - 6(1 + 3b)bc < 0.$$

Proof The equations of motion for the averaged system are

$$\begin{aligned} \dot{x}_1 &= vX_1 + \frac{b}{\sqrt{2}}X_1^2 + \frac{c + x_1^2 + (3c + X_1^2)b}{2\sqrt{2}}, \\ \dot{X}_1 &= -\left(\frac{X_1}{\sqrt{2}} + v\right)x_1. \end{aligned} \tag{18}$$

By setting the equations to zero, the equilibrium points result to be

$$\begin{aligned}
 E_{1,2} &\equiv \left(\pm\sqrt{(4-6b)v^2 - (1+3b)c}, -\sqrt{2v} \right), \\
 E_{3,4} &\equiv \left(0, \frac{-2v \pm \sqrt{4v^2 - 6(1+3b)bc}}{3\sqrt{2}b} \right).
 \end{aligned}
 \tag{19}$$

The statement of the theorem follows in a straight manner from Theorem 2 (Reeb’s theorem), provided that, under the conditions of the items, the equilibria, when they exist, are non degenerate. We name the families of periodic orbits $\gamma_i, i = 1, \dots, 4$, where the subindex indicates the corresponding orbit is associated to the equilibrium point E_i , with the same subindex. \square

It is worth noting that Eq. (18) are the same as the ones obtained by means of the classical averaging method as it was done in [17], but there the process to get them is more intricate.

The case $b = 0$ deserves a special treatment because, for this concrete value, one of the points $E_{3,4}$ goes to infinity, while the other remains, and the maximum number of equilibrium points is, therefore, three. More precisely, if $v > 0$, E_4 (minus sign) goes to infinity, whereas, if $v < 0$, it is E_3 (plus sign) which goes to infinity. Just in the case $b = 0$ we find the three equilibrium points

$$E_{1,2} \equiv \left(\pm\sqrt{4v^2 - c}, -\sqrt{2v} \right), \quad E_3 \equiv \left(0, \frac{-c}{2\sqrt{2}v} \right),
 \tag{20}$$

where we have named as E_3 the third equilibrium, regardless of whether it comes from E_3 or E_4 . Thus, by virtue of Theorem 2, we arrive at the following result.

Theorem 5 *Let us consider the Hamiltonian system defined by (17) when $\omega \approx 1$ and let K , given by (16), its average. Then, for $b = 0$ and h small enough (i.e. c small enough), there are three families of periodic orbits, parameterized by h , if $4v^2 - c > 0$. In the case the inequality reverses, there only exist a family of periodic orbits.*

The existence of periodic solutions is not the only consequence of the application of Reeb’s theorem. Indeed, the orbital stability of the periodic orbits is inherited from the parametric stability of the equilibrium points [23], which, for one degree of freedom systems, follows from the eigenvalues of the corresponding Jacobian matrix. Hence, our next task is to perform the stability analysis, which is summarized in the next theorem.

Theorem 6 *For $b \neq 0$, the families of periodic orbits $\gamma_{1,2}$ are unstable, when they exist. On the other hand we get:*

1. *If $v > 0$, $4v^2 - 6(1+3b)bc > 0$ and $(4-6b)v^2 - (1+3b)c > 0$, the family γ_3 is orbitally stable, whereas the family γ_4 is unstable for $b < 0$ and orbitally stable for $b > 0$.*
2. *If $v > 0$, $4v^2 - 6(1+3b)bc > 0$ and $(4-6b)v^2 - (1+3b)c < 0$, the two families $\gamma_{3,4}$ are unstable for $b < 0$. If $0 < b < 1/3$, then the family γ_3 is orbitally stable whereas the family γ_4 is unstable. If $b > 1/3$ the family E_3 is unstable and the family γ_4 orbitally stable.*
3. *For $v < 0$ the stability of the families γ_3 and γ_4 is as in the previous items, interchanging the indices.*

Proof We only have to accomplish the stability of the equilibrium points associated with the periodic orbits. Thus, linearizing the equations of motion (18) around an equilibrium point (x_1^0, X_1^0) , the stability character is deduced from the eigenvalues of the matrix

$$A = \begin{pmatrix} \frac{x_1^0}{\sqrt{2}} & v + \frac{3bX_1^0}{\sqrt{2}} \\ -v - \frac{X_1^0}{\sqrt{2}} & -\frac{x_1^0}{\sqrt{2}} \end{pmatrix},$$

(x_1^0, X_1^0) being the coordinates of the equilibrium point. For $E_{1,2}$ we obtain the eigenvalues

$$\lambda_{1,2} = \pm \frac{\sqrt{(4 - 6b)v^2 + (1 + 3b)c}}{\sqrt{2}}.$$

Provided these points exist when the expression into the square root is positive, they are unstable saddles and, consequently, the families $\gamma_{1,2}$ are unstable.

To establish the stability of the points $E_{3,4}$ we note that the matrix A at these points has the form

$$A|_{E_3} = \begin{pmatrix} 0 & \alpha \\ \beta & 0 \end{pmatrix}, \quad A|_{E_4} = \begin{pmatrix} 0 & -\alpha \\ \gamma & 0 \end{pmatrix},$$

where

$$\alpha = \frac{\sqrt{4v^2 - 6(1 + 3b)bc}}{2}$$

and β and γ satisfy:

$$\begin{aligned} \beta\gamma &= -\frac{(4 - 6b)v^2 - (1 + 3b)c}{6b}, \\ \beta + \gamma &= \frac{2(1 - 3b)v}{3b}, \quad \beta - \gamma = -\frac{\sqrt{4v^2 - 6(1 + 3b)bc}}{3b}. \end{aligned} \tag{21}$$

We note that α is positive and the stability character depends on the signs of β and γ . In this way, if $\beta < 0$ and $\gamma > 0$, E_3 and E_4 are stable centers. On the other hand, if $\beta > 0$ and $\gamma < 0$ the equilibrium points are unstable saddles. However, the signs of β and γ can be deduced from (21). Indeed, in the conditions of item (1), if $b < 0$ we have $\beta\gamma > 0$ and $\beta + \gamma < 0$. Thus, both β and γ are negative and, consequently, E_3 , and also the family γ_3 , is stable and E_4 and the family γ_4 unstable. On the contrary, if $b > 0$, it is deduced from (21) that $\beta\gamma < 0$, whereas $\beta - \gamma < 0$. Thus, $\beta < 0$ and $\gamma > 0$ and both E_3 and E_4 and the corresponding families $\gamma_{3,4}$ are stable.

The other two items are proved in a similar way using the relations (21) and, for the sake of conciseness, we omit the details. □

5 Bifurcations and Poincaré Surfaces of Section

As a consequence of Theorem 6, the parameter plane (b, c) is divided into different regions where the number of equilibrium points and their stability character changes. In fact, we have to distinguish the cases $v > 0$ and $v < 0$ but, by item (3) of Theorem 6, the only difference is a permutation of the indices 3 and 4. Figure 1 summarizes the results of the previous theorem for the case $v > 0$. It can be seen that there exist seven different regions, where the phase flow changes. Moreover, a bifurcation takes place when passing from one region to another limiting one. The seven regions in Fig. 1 are delimited by three curves:

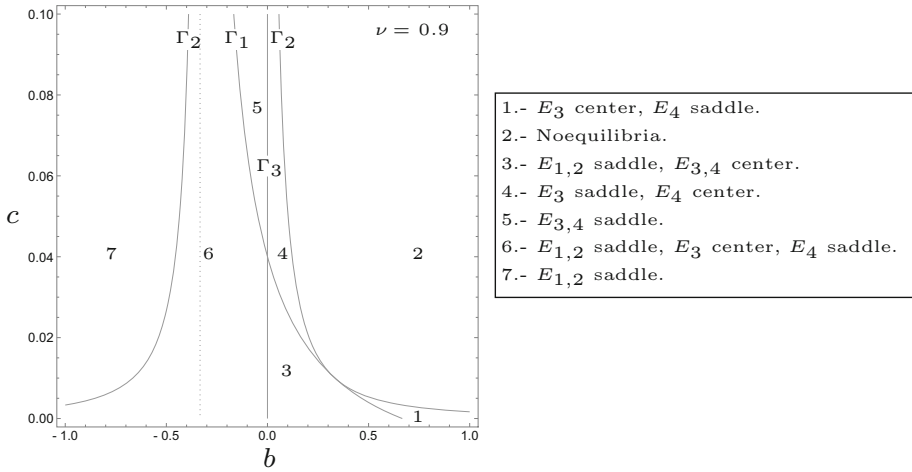
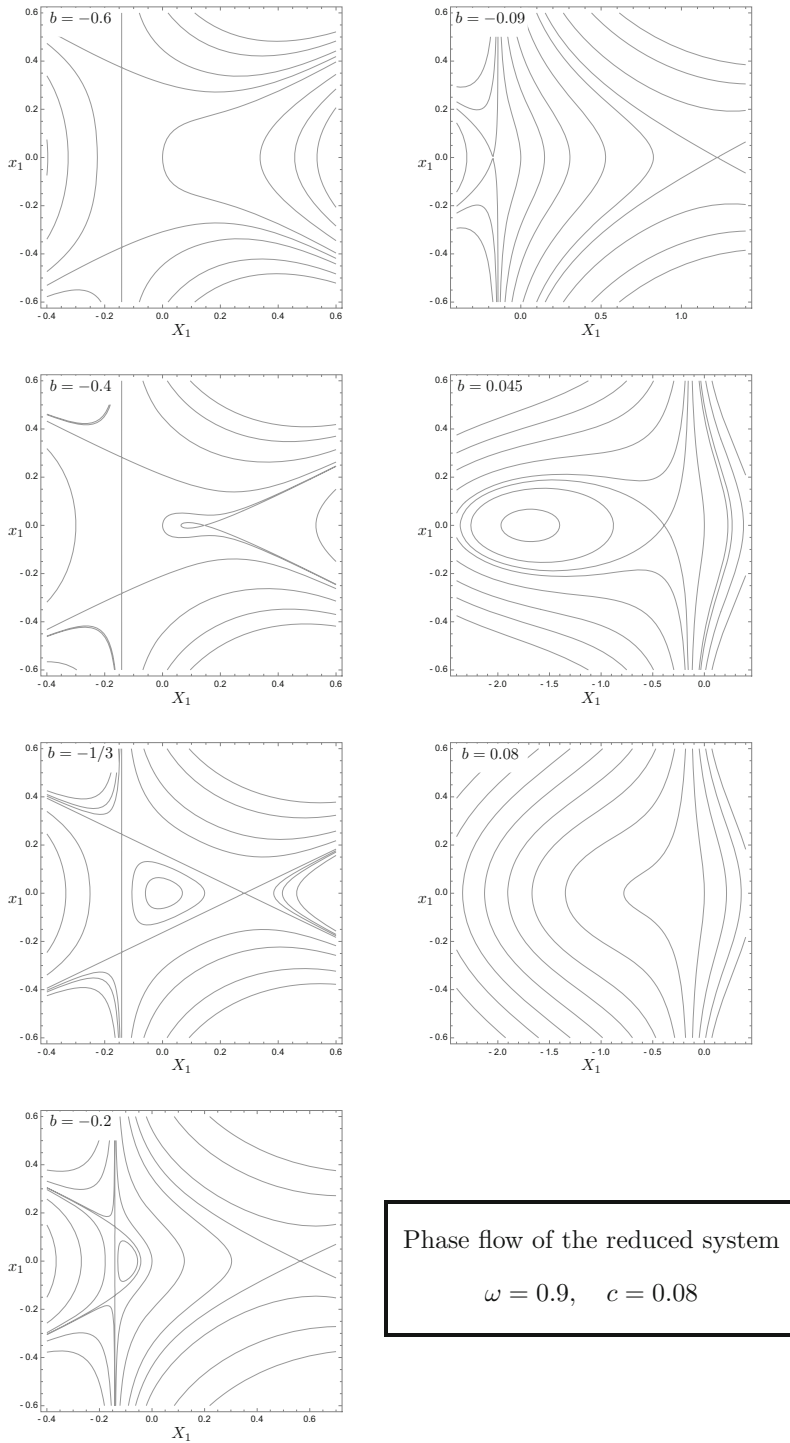


Fig. 1 The bifurcation parameter plane (b, c) for $\nu > 0$. There are seven different regions with a different type of flow

$$\begin{aligned} \Gamma_1 &\equiv (4 - 6b)\nu^2 + (1 + 3b)c = 0, \\ \Gamma_2 &\equiv 4\nu^2 - 6(1 + 3b)bc = 0, \\ \Gamma_3 &\equiv b = 0. \end{aligned}$$

The first two curves, Γ_1 and Γ_2 establish the zones where $E_{1,2}$ and $E_{3,4}$ exist, respectively. If they are crossed, the number of equilibria changes, but also the stability of the remaining points. The third one, Γ_3 , is also related to the existence of equilibrium points. In fact, when this curve is reached, one of the equilibrium points E_3 or E_4 goes to infinity and the number of equilibria reduces by one. Moreover, a change in the stability in one of these points takes place. It is worth noting that Γ_2 is asymptotic to Γ_3 . In addition, both Γ_1 and Γ_2 are asymptotic to $b = -1/3$, the classical case of the Hénon–Heiles system, which corresponds to the dotted line in Fig. 1. This is not a bifurcation line but, for $b = -1/3$, the three saddles in region 6 have the same energy and are connected by heteroclinic orbits.

In order to compare the phase flow of the reduced system with the phase flow of the original one, we set $\varepsilon = 1$ in such a way that $\nu = 1 - \omega$, and the correspondence between the two systems is clearer, taking into account that $c = h/(1 + \omega)$. We note that ε does not need to be small. The only important thing is to ensure that \mathcal{H}_1 is small in comparison with \mathcal{H}_0 , which is true if $\omega \approx 1$ and $\|(x_j, X_j)\| < 1$. Now, we fix the values of $\omega = 0.9$ and $h = 0.15$ which gives $c \approx 0.08$. We will follow the evolution of the flow as b goes from region 7 to region 2, crossing regions 6, 5 and 4. In Fig. 2 it can be observed that, for $b = -0.6$, inside the region 7, there are two saddles. As b increases and reaches region 6, a saddle-node bifurcation occurs and a new saddle and a center appear, as it is seen in Fig. 2 for $b = -0.4$. For the special value $b = -1/3$, still in region 6, the three saddles are connected and, as soon this value is overpassed, the center and the two symmetric saddles tend to coalesce ($b = -0.2$ in Fig. 2) and a subcritical pitchfork bifurcation takes place when b reaches Γ_1 . Once in region 5 ($b = -0.09$ in Fig. 2), we are left with two saddle points, namely E_3 and E_4 . As b increases, but still being negative, the saddle in the right ($X_1 > 0$) migrates to infinity and it appears as a center with $X_1 < 0$ when $b > 0$ ($b = 0.045$ in Fig. 2). Finally, when Γ_2 is crossed, a new saddle center bifurcation takes place and, in region 2, there are not critical points ($b = 0.08$ in Fig. 2).



Phase flow of the reduced system
 $\omega = 0.9, \quad c = 0.08$

Fig. 2 Evolution of the phase flow of the reduced system for $c = 0.08$, $\omega = 0.9$ and b varying from -0.6 to 0.08

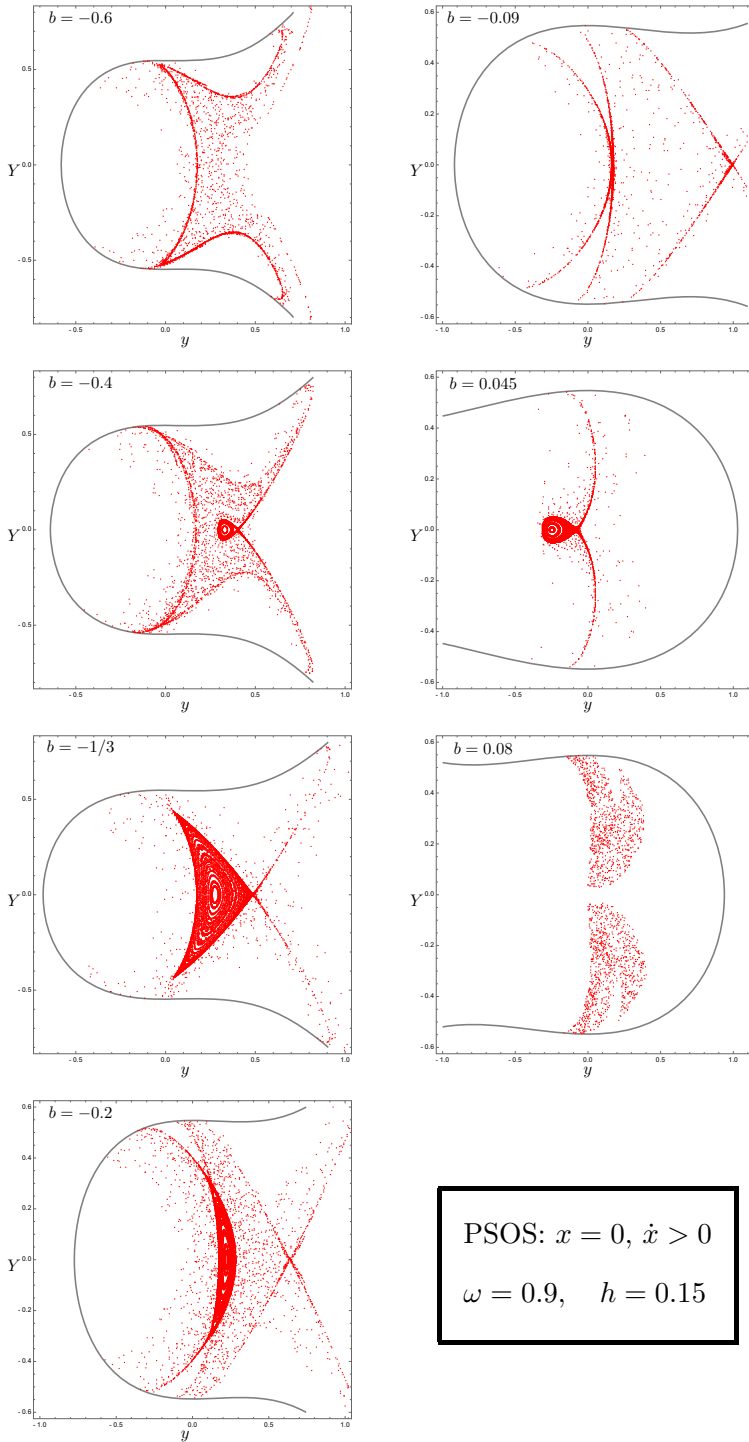


Fig. 3 Poincaré surfaces of section for the original system for $h = 0.15, \omega = 0.9$ and b varying from -0.6 to 0.08

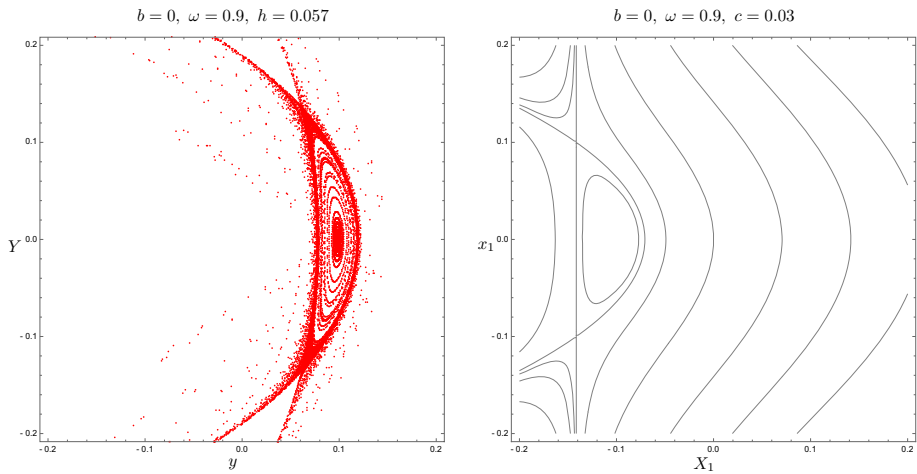


Fig. 4 Poincaré surface of section and reduced flow for $b = 0$ in the limit of regions 6 and 3

The same pattern of bifurcations is observed for the periodic orbits in the system defined by Hamiltonian (17). This is visualized by means of Poincaré surfaces of section. We start by defining the cross section $x = 0$ when it is crossed with positive velocity, that is $\dot{x} > 0$. We set $h = 0.15$ and $\omega = 0.9$ and follow the evolution of the phase flow on the surfaces of section for the same values of b taken in the reduced system. Now, periodic orbits intersect the cross section in one point and they resemble critical points. Figure 3 shows the different Poincaré surfaces of section for the specified values of b and the correspondence with the phase flow of the reduced system is clear. It is worth noting that the limit of the Poincaré surface of section undergoes a change as b crosses from negative to positive values. Indeed, the change starts at

$$b = b_0 = -\frac{(1 - \omega^2)^{3/2}}{3\sqrt{6h}},$$

when the region enclosed by the limit curve of the cross section splits into two different ones. One of them is a bounded region surrounding the origin, while the other one is an unbounded region increasingly away from the bounded one as b approaches 0. For $b = 0$ only the bounded region remains and, as soon as b takes positive values, the unbounded region appears in the other part of the cross section. The two regions merge again for $b = -b_0$. For $|b| < |b_0|$ it is not clear that the two systems look the same, because one of the equilibrium points of the reduced system blows up and the smallness required in Theorem 4 is not guaranteed. However, in the bounded region, the two systems behave in a similar way. This can be seen in Fig. 4, where a comparison between the two systems is made for $b = 0$, $\omega = 0.9$ and $h = 0.057$, which correspond to $c = 0.03$, that is in the boundary of regions 6 and 3, on the curve Γ_3 .

As it has been observed in the previous paragraphs and in Figs. 2 and 3, the behavior experienced by the equilibria of the reduced system translates to the behavior of the related periodic solutions corresponding to the full system defined in (2). In other words, the bifurcations occurring for the equilibria E_i , $i = 1, \dots, 4$ at the parametric curves Γ_1, Γ_2 render the same for the families of periodic orbits of the full Hamiltonian system. Indeed, the theory of averaging ensures that if an equilibrium point is a saddle, the family of periodic orbits

reconstructed from it is hyperbolic, see [32]. A Hamiltonian version of this is based on Reeb's theorem. In particular, the characteristic multipliers of a periodic solution are obtained from the eigenvalues of the linearization of the equilibrium, see for instance [36], specifically Corollary 2.2. Regarding the pattern followed by the bifurcations, it is also the case that a saddle-center bifurcation concerning equilibrium points is reconstructed as a saddle-center bifurcation of the resulting periodic orbits. This appears, for instance, in Ref. [12] (Theorem 3.1) and in [24] (concretely, in Theorem 6.2), although the first results on this refer to Meyer [22]. The same occurs with other bifurcations of periodic solutions reconstructed from bifurcations of equilibrium points corresponding to a reduced space, as the pitchfork bifurcation, see for instance Chapter 3 of [12]. This is realized in the following result.

Theorem 7 (1) For $v \neq 0$ a periodic Hamiltonian (subcritical) pitchfork bifurcation takes place for the periodic orbits γ_1 and γ_2 when $\Gamma_1 \approx 0$. (2) For $v \neq 0$ a periodic Hamiltonian saddle-node bifurcation takes place for the periodic orbits γ_3 and γ_4 when $\Gamma_2 \approx 0$.

Proof The proof follows straightforwardly applying the results in [12,22,24] which relates, under customary conditions of non-degeneracy (see for instance [24]), the bifurcations occurring among relative equilibrium points with the bifurcations among the associated families of periodic orbits of the corresponding full system. \square

Another interesting consequence of the relation between the relative equilibria and the families of periodic orbits is the existence of heteroclinic connections, when the equilibrium points attain the same value of the Hamiltonian function. Thus, one expects to have heteroclinic connections for the families $\gamma_{1,2}$, when they exist, and also a heteroclinic connection for the three periodic orbits sharing the same value of the Hamiltonian function for the case $b = -1/3$. In this sense, it is possible to find orbits surrounding one periodic orbit, going next to another one and surround it for a number of times and so forth. Taking as a starting orbit the naive approximation given by (10), a grid search algorithm [21], combined with the symmetries (3), is used to get the actual periodic orbits. We do that for two concrete examples, when $h = 0.08$, $\omega = 0.9$, $a = 1$ and $b = -0.6$ and $b = -1/3$. In the first case ($b = -0.6$) there are two unstable periodic orbits, symmetric respect to the y axis, which are heteroclinic connected. In the left panel of Fig. 5 the two unstable periodic orbits are depicted in bold together with an orbit that, after 15 loops around the orbit in the left, moves to the periodic orbit in the right and surrounds it 45 times before it escapes to infinity, due to the high instability character of the symmetric periodic orbits. For the case $b = -1/3$, we have the classical Hénon–Heiles system, plus the Coriolis term, which is invariant under the action of the dihedral group D_3 . Thus, the three unstable periodic orbits are equivalent excepting a $2\pi/3$ rotation about the origin and there exists a heteroclinic connection between them. In the right panel of Fig. 5 we depict the three unstable periodic orbits in bold and an orbit that goes, after 30 revolutions, from the upper periodic orbit to the left down periodic orbit. After 30 loops around it, the orbit moves to the right down periodic orbit, that also surrounds 30 times, to return again to the upper one. This cycle is repeated at least 36 times before the orbit escapes to infinity. This is an interesting phenomenon that can account for transport mechanisms in specific dynamical systems.

6 Conclusions

We have proved the existence of periodic orbits for a Hénon–Heiles rotating potential by means of the application of Reeb's theorem, which yields equivalent results to the classical

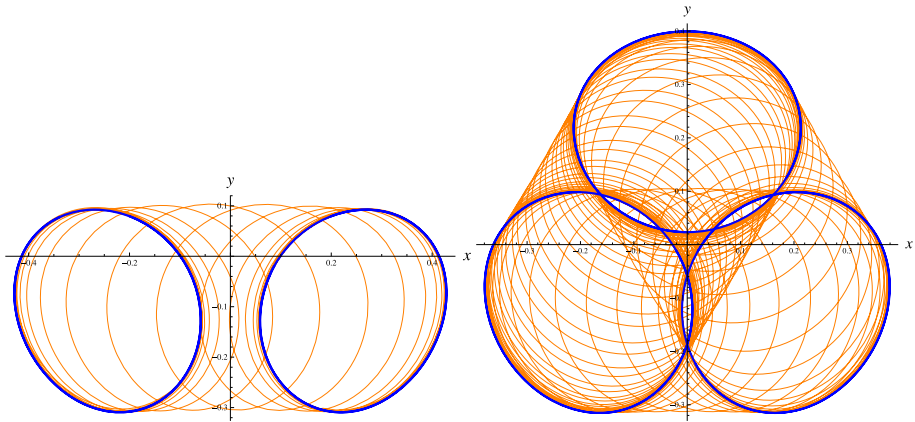


Fig. 5 Orbits close to heteroclinic connections between orbits sharing the same value of the Hamiltonian function. On the left $b = -0.6$ and on the right $b = -1/3$. In both cases $\omega = 0.9$ and $h = 0.08$

averaging method. However, it is simple to apply and techniques of reduction of polynomial Hamiltonians can be used to reduce the system to an appropriate base space, where equilibrium points are directly related to periodic solutions. Moreover, for this particular system, the equilibrium solutions and their bifurcations are, in essence, inherited by the reduced system, when the energy is small enough. This fact serves to know, in advance, that the maximum number of families of periodic orbits, around the origin, is four. Also the bifurcations we find are of saddle-center and subcritical pitchfork type, which are reconstructed to bifurcations of periodic orbits corresponding to the original Hamiltonian system. Finally, heteroclinic connections between relative equilibria translate to heteroclinic connections between periodic orbits, allowing a transport mechanism along some parts of the phase space.

Acknowledgements This work has been partly supported from the Spanish Ministry of Science and Innovation through the Projects MTM2014-59433-CO (Subprojects MTM2014-59433-C2-1-P and MTM2014-59433-C2-2-P), MTM2017-88137-CO (Subprojects MTM2017-88137-C2-1-P and MTM2017-88137-C2-2-P), and by University of La Rioja through Project REGI 2018751.

References

1. Alfaro, F., Llibre, J., Pérez-Chavela, E.: Periodic orbits for a class of galactic potentials. *Astrophys. Space Sci.* **344**, 39–44 (2013)
2. Arnold, V.: On matrices depending on parameters. *Russ. Math. Surv.* **26**, 29–43 (1971)
3. Binney, J., Tremaine, S.: *Galactic Dynamics*. Princeton University Press, Princeton (1994)
4. Blesa, F., Seoane, J.M., Barrio, R., Sanjuán, M.A.F.: To escape or not to escape, that is the question—perturbing the Hénon–Heiles Hamiltonian. *Int. J. Bifurcat. Chaos.* **22**, 1230010 (2012)
5. Carrasco-Olivera, D., Uribe, M., Vidal, C.: Periodic orbits associated to Hamiltonian functions of degree four. *J. Nonlinear Math. Phys.* **21**, 336–356 (2014)
6. Corbera, M., Llibre, J., Valls, C.: Periodic orbits of perturbed non-axially symmetric potentials in 1:1:1 and 1:1:2 resonances. *Discrete Cont. Dyn. B.* **23**, 2299–2337 (2018)
7. Cushman, R., Kelley, A., Koçac, H.: Versal normal form at the Lagrange equilibrium L_4 . *J. Differ. Equ.* **64**, 340–374 (1986)
8. Elmandouh, A.A.: On the dynamics of Armbruster–Guckenheimer–Kim galactic potential in a rotating reference frame. *Astrophys. Space Sci.* **361**, 182 (2016)

9. El-Dessoky, M.M., Elmandouh, A.A., Hobiny, A.: Periodic orbits of the generalized Friedman–Robertson–Walker potential in galactic dynamics in a rotating reference frame. *AIP Adv.* **7**, 035021 (2017)
10. de Zeeuw, T., Merritt, D.: Stellar orbits in a triaxial galaxy I. Orbits in the plane of rotation. *Astrophys. J.* **267**, 571–595 (1983)
11. Gerhard, O.E., Saha, P.: Recovering galactic orbits by perturbation theory. *Mon. Not. R. Astr. Soc.* **251**, 449–467 (1991)
12. Hanßmann, H.: Local and Semi-Local Bifurcations in Hamiltonian Dynamical Systems: Results and Examples. *Lecture Notes in Mathematics*, vol. 1893. Springer, Berlin (2007)
13. Hénon, M., Heiles, C.: The applicability of the third integral of motion: some numerical experiments. *Astron. J.* **69**, 73–79 (1964)
14. Iñarrea, M., Lanchares, V., Palacián, J.F., Pascual, A.I., Salas, J.P., Yanguas, P.: Lyapunov stability for a generalized Hénon–Heiles system in a rotating reference frame. *Appl. Math. Comput.* **253**, 159–171 (2015)
15. Kawai, S., Bandrauk, A.D., Jaffé, C., Bartsch, T., Palacián, J.F., Uzer, T.: Transition state theory for laser-driven reactions. *J. Chem. Phys.* **126**, 164306 (2007)
16. Lanchares, V., Pascual, A.I., Palacián, J.F., Yanguas, P., Salas, J.P.: Perturbed ion traps: a generalization of the three-dimensional Hénon–Heiles system. *Chaos* **12**, 87–99 (2002)
17. Lanchares, V., Iñarrea, M., Palacián, J., Pascual, A.I., Salas, J.P., Yanguas, P.: Periodic solutions in the Hénon–Heiles rotating system. *Monografías Matemáticas García de Galdeano* **42**, 165–172 (2019)
18. Llibre, J., Jiménez-Lara, L.: Periodic orbits and non-integrability of Hénon–Heiles systems. *J. Phys. A Math. Theor.* **44**, 205103 (2011)
19. Llibre, J., Paşca, D., Valls, C.: Periodic solutions of a galactic potential. *Chaos Soliton Fract.* **61**, 38–43 (2014)
20. Llibre, J., Vidal, C.: Periodic motion in non-axially symmetric galaxies. *J. Geom. Phys.* **140**, 1–99 (2019)
21. Markellos, V., Black, W., Moran, P.: A grid search for families of periodic orbits in the restricted problem of three bodies. *Celest. Mech.* **9**, 507–512 (1974)
22. Meyer, K.R.: Generic bifurcation of periodic points. *Trans. Am. Math. Soc.* **149**, 95–107 (1970)
23. Meyer, K.R., Palacián, J.F., Yanguas, P.: Geometric averaging of Hamiltonian systems: periodic solutions, stability, and KAM tori. *SIAM J. Appl. Dyn. Syst.* **10**, 817–856 (2011)
24. Meyer, K.R., Palacián, J.F., Yanguas, P.: Singular reduction of resonant Hamiltonians. *Nonlinearity* **31**, 2854–2894 (2018)
25. Palacián, J.F., Yanguas, P.: Reduction of polynomial Hamiltonians by the construction of formal integrals. *Nonlinearity* **13**, 1021–1054 (2000)
26. Palacián, J.F., Yanguas, P.: Reduction of polynomial Hamiltonians with quadratic unperturbed part. *SIAM Rev.* **42**, 671–691 (2000)
27. Patsis, P.A., Harsuola, M.: Building CX peanut-shaped disk galaxy profiles. The relative importance of the 3D families of periodic orbits bifurcating at the vertical 1:2 resonance. *A&A* **612**, A114 (2018)
28. Pucacco, G., Bocaletti, D., Belmonte, C.: Quantitative predictions with detuned normal forms. *Celest. Mech. Dyn. Astron.* **102**, 163–176 (2008)
29. Ramilowski, J.A., Prado, S.D., Borondo, F., Farrelly, D.: Fractal Weyl law behavior in an open Hamiltonian system. *Phys. Rev. E* **80**, 055201(R) (2009)
30. Reeb, G.: Sur certaines propriétés topologiques des trajectoires des systèmes dynamiques. *Acad. R. Belgique. Cl. Sci. Mém. Coll. in 8°*. 27 article 9 (1952)
31. Romero-Gómez, M., Masdemont, J.J., García-Gómez, C., Athanassoula, E.: The role of the unstable equilibrium points in the transfer of matter in galactic potentials. *Commun. Nonlinear Sci.* **14**, 4123–4138 (2009)
32. Sanders, J.A., Verhulst, F., Murdock, J.: *Averaging Methods in Nonlinear Dynamical Systems*, 2nd edn. Springer, New York (2007)
33. Schmidt, D.: Versal normal form of the Hamiltonian function of the restricted problem of three bodies near \mathcal{L}_4 . *J. Comput. Appl. Math.* **52**, 155–176 (1994)
34. Tuwankotta, J.M., Verhulst, F.: Hamiltonian systems with widely separated frequencies. *Nonlinearity* **16**, 689–706 (2003)
35. Verhulst, F.: *Nonlinear Differential Equations and Dynamical Systems*. Springer, New York (1990)
36. Yanguas, P., Palacián, J.F., Meyer, K.R., Dumas, H.S.: Periodic solutions in Hamiltonian systems, averaging, and the lunar problem. *SIAM J. Appl. Dyn. Syst.* **7**, 311–340 (2008)